Self-Healing in Power Systems: An Approach Using Islanding and Rate of Frequency Decline-Based Load Shedding

Haibo You, *Student Member, IEEE*, Vijay Vittal, *Fellow, IEEE*, and Zhong Yang

***Abstract*—This paper provides a self-healing strategy to deal with catastrophic events when power system vulnerability analysis indicates that the system is approaching an extreme emergency state. In our approach, the system is adaptively divided into smaller islands with consideration of quick restoration. Then, a load shedding scheme based on the rate of frequency decline is applied. The proposed scheme is tested on a 179-bus, 20-generator sample system and shows very good performance.**

***Index Terms*—Islanding, load shedding, self-healing, slow-coherency-based grouping.**

I. Introduction

POWER SYSTEMS are being operated closer to the stability limit nowadays as deregulation introduces more economic objectives for operation. As open-access transactions increase, weak connections, unexpected events, hidden failures in protection system, human errors, and other reasons may cause the system to lose balance and even lead to catastrophic failures. Iowa State University, together with University of Washington, Virginia Polytechnic Institute and State University, and Arizona State University have worked as a consortium to conduct research on power system network security issues. The project is being conducted under a grant from the Electric Power Research Institute (EPRI) and the U.S. Department of Defense (DoD). One of the tasks involves the development of self-healing schemes for power systems. This paper addresses the topic of designing a self-healing strategy after large disturbances. When a power system is subjected to large disturbances, such as simultaneous loss of several generating units or major transmission lines, and the vulnerability analysis indicates that the system is approaching a catastrophic failure, control actions need to be taken to limit the extent of the disturbance. In our approach, the system is separated into smaller islands at a slightly reduced capacity. The basis for forming the islands is to minimize the generation-load imbalance in each island, thereby facilitating the restoration process. Then, by exploring a carefully designed load shedding scheme based on the rate of frequency decline, we limit the extent of the disruption, and are able to restore the system rapidly. We refer to this corrective control scheme as controlled islanding followed by load shedding based on the rate of frequency decline.

Subsumption architecture [1], which is used in the field of controlled robots, is adopted here to identify the hierarchies of the various controls, protection, and communication systems between various agents in the deregulated electric utility environment. The architecture is based on the premise that storing models of the world is dangerous in dynamic and unpredictable environments because representations may be incorrect or outdated. It defines layers of finite-state machines (FSMs) that are augmented with timers. Sensors feed information into FSMs at all levels. The FSMs of the lowest level are control actuators. The FSMs of the higher levels may inhibit (attenuate the signal of one output wire) or suppress (attenuate the signal on all output wires) output values of the FSMs on the layers below them. In this way, a hierarchy of progressively refined behaviors may be established. Agents designed using the subsumption architecture do not use symbol manipulation in a fixed manner to represent processing. They also have no global knowledge and are generally decentralized. The agents are nonprogrammable, single-purpose devices due to their lack of symbolism and global knowledge. However, they have the advantage of rapid response for dealing with dynamic and unpredictable events. A load shedding scheme based on the subsumption model is designed with consideration of certain criteria. The proposed scheme is tested on a 179-bus 20-generator test system and shows very good performance.

II. Controlled Islanding

In this step, we employ a two-time-scale method to determine the groups of the generators with slow coherency. This method considers the structural characteristics of the power system to determine the interactions of the various generators and find the strong and weak couplings. The method is implemented by running the Dynamic Reduction Program 5.0 (DYNRED) software obtained from the EPRI software center. Through the selection of the two-time-scale option, the coherent groups of generators can be obtained on any power system. We also develop an automatic islanding program to fully support the application of the theory.

A. Slow Coherency

In the controlled islanding self-healing approach, the determination of the islands for a given operating condition is the critical step. A reasonable approach to islanding can result in

Manuscript received March 21, 2002; revised June 26, 2002. This work was supported by the U.S. Department of Defense and Electric Power Research Institute through the Complex Interactive Networks/Systems Initiative WO 8333-01.

H. You and V. Vittal are with the Department of Electrical and Computer Engineering, Iowa State University, Ames, IA 50010 USA.

Z. Yang is with GE Power and Energy System, Melbourne, FL 32935 USA.

Digital Object Identifier 10.1109/TPWRS.2002.807111

significant benefit to the corrective control actions that follow the islanding procedure. In determining the islands, the inherent structural characteristics of the system should be considered. In addition, the choice of these islands should not be disturbance dependent. The two-time-scale method we employed is an application of the singular perturbation method in power systems [2]–[4]. The method assumes the state variables of an nth order system are divided into r slow states y, and (n–r) fast states z, in which the r slowest states represent r groups with the slow coherency. The user provides an estimate for the number of groups. However, the automatic islanding program takes into account the mismatch between generation and load and availability of the tie lines to form islands and appropriately combines groups when islands cannot be formed. Both the linearized and nonlinear power system models can be used to apply the two-time-scale method. In the linearized model, we start from the basic classical second-order electromechanical model of an n-machines power system [5]:

$$\dot{\delta}_i = \Omega(\omega_i - 1) \tag{1}$$

$$2H_i\dot{\omega}_i = -D_i(\omega_i - 1) + (P_{mi} - P_{ei}) \quad i = 1, 2, \ldots, n \tag{2}$$

where

- δ_i rotor angle of machine i in radians;
- ω_i speed of machine i, in per unit;
- P_{mi} mechanical input power of machine i, in per unit;
- P_{ei} electrical output power of machine i, in per unit;
- H_i inertia constant of machine i, in seconds;
- D_i damping constant of machine i, in per unit;
- Ω base frequency, in radians per second.

If we neglect damping and line conductance and we linearize the system dynamic equation around an equilibrium point $(\delta^*, 1)^T$, we obtain

$$\ddot{X} = -(1/2)\Omega H^{-1}KX = AX \tag{3}$$

$$x_i = \Delta\delta_i \qquad i = 1, 2, \ldots, n \tag{4}$$

$$H = \mathrm{diag}(H_1, H_2, \ldots, H_n) \tag{5}$$

$$K = (k_{ij}) = (V_iV_jB_{ij}\cos(\delta_i - \delta_j)|_{\delta^*}) \qquad j \neq i \tag{6}$$

where V_i voltage of bus i (per unit), B_{ij} prefault network's susceptance between bus i and bus j.

Further transformations based on this simplified model are made. It is to be noted that this model retains all of the oscillation frequency information. In the case that a Riccati equation is satisfied, slow and fast variables of the system are classified through a proper grouping algorithm. The detailed description of the method can be found in [3]–[6].

As a summary, the slow coherency based grouping method has the following explicit advantages.

1) Slow coherency is independent of initial condition and disturbance.
2) The two-time-scale weak connection form inherently describes the oscillation feature of large-scale power systems: the fast oscillation within a group of machines and the slow oscillation between the groups via weak tie lines.
3) The slow coherency method also preserves the features of the coherency-based grouping. It is independent of the size of the disturbance and the generator model detail.

The technique is implemented by running DYNRED. Through the selection of the two-time-scale option, the coherent groups of generators can be obtained on any power system. The islands are formed by slow coherency considering the modes of the oscillation of the linearized state space model of the system. This is reasonable since the islands contain the generators with similar swing characteristics and oscillation frequencies that are unrelated with the size and the location of the disturbance. It is also reasonable to assume that the same group of generators will show similar behavior (slow coherency) following the disturbance. This is reasonable to assume since the automatic islanding occurs quite early after the disturbance (0.2 s after the initiation of the disturbance). We have also verified by nonlinear simulation that the grouping identified by the slow coherency approach is maintained in the nonlinear simulation beyond this time instant. It has also been observed, that in nonlinear simulations following disturbances, the fundamental modes of oscillation that describe the inherent structural characteristics of the systems can be clearly identified. Hence, the fundamental modes of the oscillation determined by the linear analysis provide a convenient approach to detect the structural characteristics of the system.

B. Islanding

Having decided the coherent groups of the generators, we still have two questions to answer. They are: Where and when to form the islands? We develop an automatic islanding program to fully support the application of theory. The program is dedicated to searching for the optimum cut sets after we have the grouping information. The optimum cut set is obtained considering the least generation-load imbalance. The approach begins with the characterization of the network structure or connectivity using the adjacent link table data structure [7]. Then through a series of reduction processes, the program forms a small network and performs an exhaustive search on it to get all the possible cut sets.

With the information of the coherent groups of generators and the exact locations of where to form the islands, the R-Rdot out of step relay developed at Bonneville Power Administration (BPA) is deployed to form the islands [8]–[9]. The relay only requires local measurements and makes tripping decision using settings based on various offline contingency simulations. It shows much better performance than the conventional out of step relay, which is actually the impedance relay. Besides the impedance, the new relay uses the information of the rate of change of the impedance or resistance and gets better results in practice. Different switching lines make sure different corrective control actions are taken based on the level of the seriousness of the disturbance. The switching lines are as shown in Fig. 1 [8], [9]. When a fault trajectory enters into the range defined by the switching lines, the tripping action will take place.

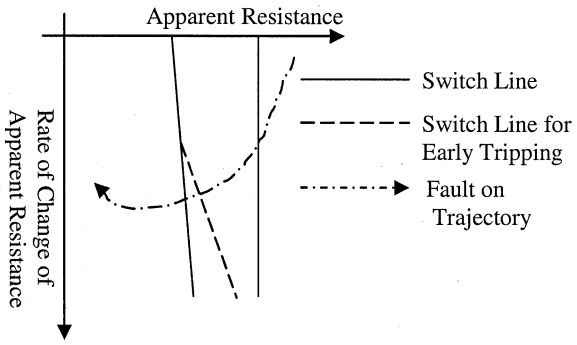

Fig. 1. R-Rdot out-of-step relay switch lines.

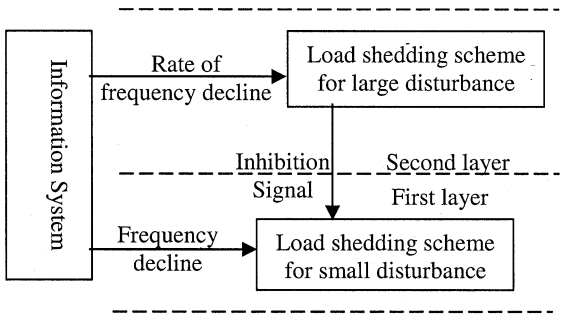

Fig. 2. Subsumption model for the load shedding scheme.

III. Load Shedding Scheme

Controlled islanding divides the power system into islands. Some of these islands are load rich and others may be generation rich. Generally, in a load rich island, the situation is more severe. The system frequency will drop because of the generation shortage. If the frequency falls below a certain set point (e.g., 57.5 Hz), the generation protection system will begin operation and trip the generator, further reducing the generation in the island and making the system frequency decline even worse. In the worst case, the entire island will blackout. In a load deficient island, either intentional or forced generator tripping will reduce the gap between the generation and the load. As a result, we put more effort to save the load rich island and develop a new two-layer load shedding scheme to perform the task [10].

A. Load Shedding Scheme Under Subsumption Model

In the literature, there exist two kinds of load shedding schemes: load shedding based on frequency decline and load shedding based on rate of frequency decline [11], [12]. The first approach [11] has mostly conservative settings because of the lack of information regarding the magnitude of the disturbance. Although this approach is effective in preventing inadvertent load shedding in response to small disturbances with relatively longer time delay and lower frequency threshold, it is not able to distinguish between the normal oscillations of the power system and the large disturbances on the power system. Thus, the approach is prone to shedding less load. This is not beneficial to the quick recovery of the island and may lead to further cascading events. The second approach [12] avoids these shortcomings by using the frequency decline rate as a measure of the load shortage. Thus, it has a faster response time compared to the other scheme.

The idea of the load shedding based on the rate of change of frequency can be traced back to as early as in 1960s [13], [14]. Issues of hardware implementations in the form of relays were discussed and resolved in the 1970s and 1980s. In [14], the leakage occurring in the fast Fourier transform (FFT) is advantageously used to detect the fluctuations in the fundamental frequency of a power system so that it can optimally estimate the mean frequency and its average rate of decline and determine the appropriate amount of load to be shed. The idea was then adopted in an isolated power system [15], [16]. In the U.K., the principal of the rate of change of frequency used for load shedding is referred to as ROCOF. In [17], an adaptive load shedding scheme that uses information including the system demand, spinning reserve, system kinetic energy, the amount of lower-priority load available for shedding elsewhere, and the locally measured rate of change of frequency is developed.

We develop a load shedding scheme based on the rate of frequency decline, which can identify the magnitude of the disturbance. At the same time, we incorporate the conventional load shedding scheme into our subsumption model to form a new two-level load shedding scheme as shown in Fig. 2.

Normally, the relay will operate the conventional load shedding scheme. The conventional load shedding scheme has longer time delays and lower frequency thresholds, which can be used to prevent inadvertent load shedding in response to small disturbances. If the system disturbance is large and exceeds the signal threshold, the second layer will be activated and send an inhibition signal to the first layer and the load shedding scheme based on the rate of frequency decline will take effect. This layer of the load shedding will shed more load quickly at the early steps to prevent the cascading events in the island. This can greatly enhance the system's ability to withstand large disturbances. In all, the new two-level load shedding scheme has the following explicit features:

1) suitable for large and small disturbances;
2) suitable for self-healing when combined with islanding in power system recovery.

B. Determination of the Magnitude of the Disturbance

A variable that measures the magnitude of the disturbance should be determined in order to make the subsumption approach feasible. From an intuitive analysis [18], the rate of frequency decline at the beginning of the disturbance can accurately reflect the magnitude of the disturbance. From [19, chapter 3], we have

$$\frac{df_i}{dt} = -\frac{60 \times P_{sik}}{2H_i}\left(P_{L\Delta}(0^+) \Big/ \sum_{i=1}^{n} P_{sik}\right) \quad i = 1, 2, \ldots, n. \tag{7}$$

Define

$$\overline{f} = \sum_{i=1}^{n}(H_i f_i) \Big/ \left(\sum_{i=1}^{n} H_i\right). \tag{8}$$

In (7), we add all the equations to obtain

$$\frac{d\overline{f}}{dt} = \sum_{i=1}^{n}\left(H_i \cdot \frac{df_i}{dt}\right) \Bigg/ \sum_{i=1}^{n} H_i = -60 \times P_{L\Delta} \Bigg/ \sum_{i=1}^{n} 2H_i. \quad (9)$$

f_i frequency of generator i in hertz;
$d\overline{f}/dt$ average rate of frequency decline, in hertz per second;
P_{sik} synchronizing power coefficient between generator i and the disturbance node k, in per unit. See [19, Chapter 3];
$P_{L\Delta}$ magnitude of the disturbance, in per unit;
H_i inertia of generator i, in per unit;
ω_i rotor speed of each generator i, in per unit.

We define

$$m_i = \frac{df_i}{dt} \quad (10)$$

$$m_0 = \frac{d\overline{f}}{dt}. \quad (11)$$

Substituting (11) into (8), we have

$$m_0 = -60 \times P_{L\Delta} \Bigg/ \sum_{i=1}^{n} 2H_i. \quad (12)$$

The equation can be alternatively written as

$$P_{L\Delta} = -m_0 \times \sum_{i=1}^{n} 2H_i/60. \quad (13)$$

Since H_i is constant, the magnitude of the disturbance can be directly related to the average rate of system frequency decline. Hence, m_0 can be an indicator of the severity of the disturbance. The rate of frequency decline at the beginning of the disturbance can be used as the input signal of the second layer. Once the threshold of $P_{L\Delta}$ to activate the second layer is decided, the corresponding m_0 can be calculated. When the disturbance occurs, we measure m_i at each bus and compare it with m_0. If m_i is greater than m_0, the second layer is activated; otherwise, the conventional load shedding scheme is used.

By using m_i at each bus to decide the amount of load that should be shed locally, the system oscillations after the disturbance can be reduced. We know that at the beginning of the disturbance, the impact of disturbance is shared immediately by the generators according to their synchronizing power coefficients with respect to the bus at which the disturbance occurs [19]. Thus, the machines electrically close to the point of impact will pick up the greater share of the load regardless of their size. On the other hand, standards [20] and guides [21] give a fairly strict regulation on tolerable frequency deviations. The area between 59.5 and 60.5 Hz is the area of unrestricted time operating frequency limits. The areas above 60.5 Hz and below 59.5 Hz are areas of restricted time operating frequency limits. From Section III-C, we also note that the system frequency is not allowed to drop below 57 Hz. Hence, on detection of the system frequency dropping below 59.5 Hz, the load shedding schemes should trigger the corrective control ensuring that the system frequency will not drop below 57 Hz. Although the disturbance is ultimately shared according to the inertia of each machine, sometimes the frequency of some generators near the disturbance can drop below 57 Hz before reaching the final state. Using the value of frequency at each bus, the buses whose frequencies drop quickly are likely to have more load shed locally; this can reduce the frequency deviation and system oscillations.

C. Determination of the Threshold $P_{L\Delta}$

Considering the governor protection system limitation and regional operation criteria, we define $P_{L\Delta}$ as the minimum load deficit that can drive the system average frequency below 57 Hz. This frequency threshold is chosen because it is widely recognized that the system is not allowed to operate below 57 Hz. There are three main reasons why the system cannot operate below 57 Hz.

1) Coordination With the Governor-Turbine System: Underfrequency operating limitations imposed by manufacturers of turbine-generator units are primarily concerned with the avoidance of resonant frequencies and turbine blade fatigue. Since fatigue effects are cumulative, the limitation is defined in terms of total accumulated times of operation within specified frequency ranges. Turbine manufacturers provide limitations of various turbines to frequency variation. Based on this data, it is very reasonable to choose 57 Hz as system operation limit [18].

2) Coordination With the Plant Auxiliary System: Nuclear units having a pressurized water reactor steam supply use special underfrequency protection for their primary system reactor coolant pumps. For these units, this protection will trip the coolant pumps and shutdown the reactor at the fixed time of 0.25 s and a pickup setting of 57.0 Hz [22].

3) Coordination With Existing Operation Criteria: According to the North East Power Coordinating Council (NPCC) standard, the generation rejection should be deployed immediately if system frequency drops below 57 Hz [23].

To find $P_{L\Delta}$, we use a reduced model for a reheat unit for frequency disturbance as shown in Fig. 3 [18].

Here, K_m is a mechanical power gain factor. We use a typical value of 0.95.

H nertia constant in seconds, typically 4.0 s;
f_H high-pressure power fraction, typically 0.3;
D damping factor, typically 1.0;
T_R reheat time constant, seconds, typically 8.0 s;
R fraction of the reheat turbine, typically 0.559;
P_d disturbance power, in per unit.

We use typical system data to compute the minimum load deficit that can drive the system to the minimum frequency of 57 Hz (representing the worst-case scenario).

From Fig. 3

$$\Delta\omega = \left(\frac{R\Omega_n^2}{DR + K_m}\right)\left(\frac{(1 + T_R s)P_d}{s^2 + 2\Omega_n^2\lambda s + \Omega_n^2}\right) \quad (14)$$

where

$$\Omega_n^2 = \frac{DR + K_m}{2HRT_R} \quad (15)$$

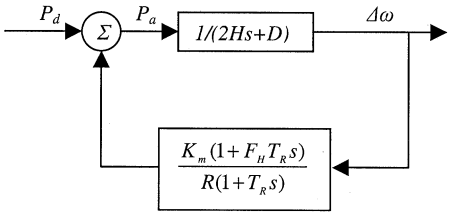

Fig. 3. Reduced model of reheat unit for frequency disturbance.

$$\lambda = \left(\frac{2HR + (DR + K_m F_H) T_R}{2(DR + K_m)} \right) \Omega_n. \tag{16}$$

If P_d is a step function, then

$$P_d(t) = P_{step} u(t). \tag{17}$$

Using this reduced model and normalizing, we obtain that the lowest system average frequency for this disturbance is 57 Hz when $P_d = P_{L\Delta} = 0.3P_{sys}$. So, we choose $0.3P_{sys}$ as the threshold value of $P_{L\Delta}$ for the new load shedding scheme. This value of $P_{L\Delta}$ is used in (13) to determine the limiting threshold for m_0.

D. Frequency Threshold, Step Size, and Time Delay

The frequency threshold should be chosen carefully. First, it should not be too close to normal frequency in order to avoid tripping on severe but nonemergency frequency swings. On the other hand, it is more effective to shed load earlier.

The step size is an important variable in load shedding. Conventionally, the amount of load shed at each step is increased while the system frequency decreases. This choice is reasonable for those schemes that use the frequency as the criterion to shed load because before the system deteriorates, it is unreasonable to shed too much load if the disturbance is unknown. It has also been observed that for large disturbances, such schemes may be insufficient to arrest system frequency decline [24]. Our second layer of load shedding scheme, as stated before will only take action when the disturbances are large enough to cause the system frequency to drop below 57 Hz. So instead of increasing the step size while the system frequency is decreasing, we set the first step to be the largest step size. This helps the system recovery in the case of large disturbance. Since the first layer of the new load shedding scheme will mainly deal with small disturbances, the conventional philosophy is adopted for this layer, or the load is shed only based on frequency decline. For the steps of load shedding, the following three facts have been observed [24].

1) Frequency steps must be far enough apart to avoid overlap of shedding due to (intentional or inherent) time delay.

2) The number of steps does not have very great impact on the effect of load shedding.

3) Generally, the threshold of the last step of load shedding is chosen no less than 58.3 Hz.

Time delay is very important for load shedding schemes to avoid overlapping and unexpected action for small frequency oscillations. Generally, for the conventional load shedding scheme, the delay time for the first step is usually very long to avoid unexpected actions due to small frequency oscillations.

TABLE I
STEP SIZE AND DELAY TIME OF THE TWO LAYERS AS PERCENTAGE OF THE TOTAL LOAD

	59.5 Hz	59.3 Hz	58.8 Hz	58.6 Hz	58.3 Hz
$m_i > m_0$	20% (0C)		5% (6C)	4% (12C)	4% (18C)
$m_i < m_0$		10% (28C)	15% (18C)		

For the following steps, the more the frequency declines, the quicker the action is. For the new scheme, to prevent sharp frequency declines following a large disturbance, we set the delay time for the first step of the second layer as zero cycles.

Finally, the two layers of load shedding scheme are developed as shown in the Table I. When the disturbance occurs, we measure m_i or the rate of frequency decline at each bus and compare it with m_0 calculated from $P_{L\Delta}$. If m_i is greater than m_0, the new load shedding scheme shown in the second row of Table I is deployed. Twenty percent of the total load is shed with zero cycle delay in the first step. The character C in the table means cycle. Otherwise, the conventional load shedding scheme is used, which is shown in the second row.

IV. SIMULATION RESULT

The load shedding scheme is tested on a 179-bus, 29-generator test system. The system has a total generation of 61 410 MW and 12 325 Mvar. It has a total load of 60 785 MW and 15 351 Mvar. The simulation is made using a detailed generator model with governors, exciters, and power system stabilizers (PSS). In the first case, the system is islanded by experience. In the second case, the DYNRED program in the PSAPAC package was chosen to form four groups of generators based on slow coherency. With the help of the automatic islanding program, we determine the cut sets of the island with consideration of the least generation-load imbalance and topology requirements. In the third case, a different fault is chosen from the previous two cases. Islands are formed based on the slow coherency approach.

In the first and the second case, to test the system response to a severe contingency, three 500-kV transmission lines in the system are tripped simultaneously shown as in Fig. 4. This corresponds to a catastrophic transmission failure where an incident takes out all three transmission lines simultaneously. The arrow shows the location where the three transmission lines are disconnected. These lines are connected between buses.

1) bus 83–bus 168;
2) bus 83–bus 170;
3) bus 83–bus 172.

Simulations conducted on the system indicate that this disturbance will result in the system being unstable. In these simulations, no conventional protection settings were considered. To save the system from an impending blackout, we split the system into two islands 0.2 s after the contingency. In the first case, **the islands are formed by experience**. The following lines are tripped:

1) bus 139–bus 12;
2) bus 139–bus 27;
3) bus 136–bus 16 (1 and 2).

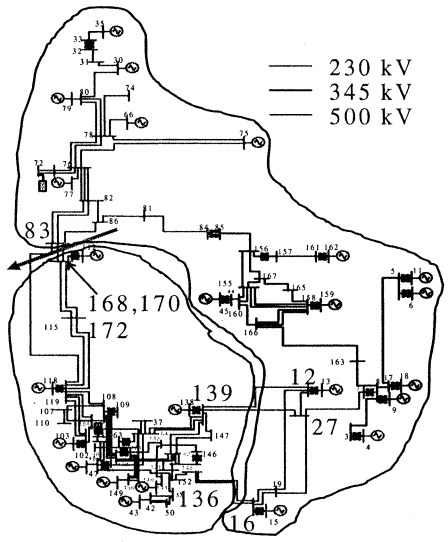

Fig. 4. Case 1—two islands for 179-bus system based on experience.

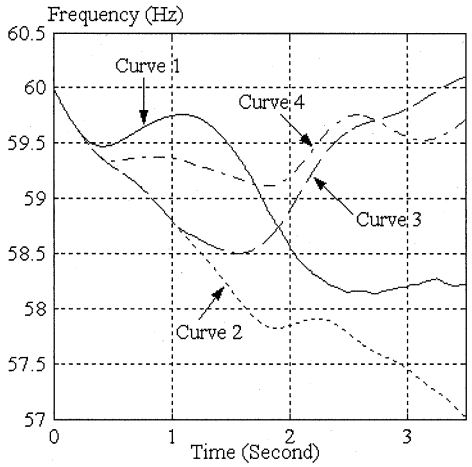

Fig. 5. Frequency response of generator 118 after the contingency of the 179-bus system. Curve 1: Without self-healing. Curve 2: Islanding with no load shedding. Curve 3: Islanding followed by load shedding based on frequency difference. Curve 4: Islanding followed by load shedding based on the rate of frequency decline.

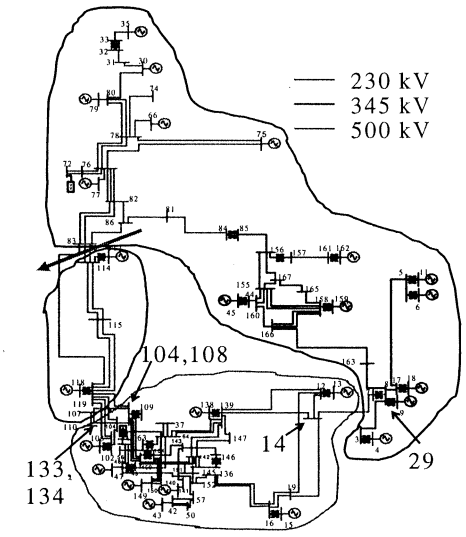

Fig. 6. Case2—three islands for 179-bus system based on slow coherency.

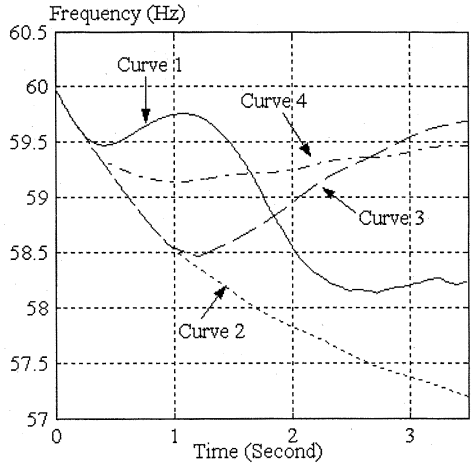

Fig. 7. Frequency response of generator 118 after the contingency of the 179-Bus system. Curve 1: Without self-healing. Curve 2: Islanding with no load shedding. Curve 3: Islanding followed by load shedding based on frequency difference. Curve 4: Islanding followed by load shedding based on the rate of frequency decline.

After islanding, the system is divided into two islands shown as in Fig. 4. The two islands can be characterized as the northeast island, which is generation rich, and the southwest island, which is load rich. In the southwest island, some of the buses have mi smaller than m_0. So the conventional load shedding scheme is deployed at these buses. For the other buses at which m_i is larger than m_0, the load shedding scheme based on the rate of frequency decline is deployed.

In the simulation, underfrequency load shedding with various schemes is performed in the southwest island to maintain acceptable frequency. Simulations are conducted using EPRI's Extended Transient-Midterm Stability Program (ETMSP). Fig. 5 shows the frequency responses of a typical generator in the southwest island in four situations.

Curve 1 and curve 2 show that, following the disturbance, the system will lose stability without any self-healing strategy or only with islanding. Curve 3 and curve 4 give a comparison between the two load shedding schemes. To maintain stability of the system, less load needs to be shed with the new load shedding scheme than the old scheme. At the same time, the system experiences smaller frequency excursions under the new scheme than the old scheme.

In determining the islands using slow coherency we specified the initial estimate of the groups to be four. Based on the grouping and the fault location in the second case, in order to create the islands for such a large disturbance, the automatic islanding program selects the following lines to be tripped:

1) bus 133–bus 108;
2) bus 134–bus 104;
3) bus 29–bus 14.

As mentioned before, the **lines are determined by the automatic islanding program. Nonlinear fault-on simulations show that the generators within the same group show coherency with each other.** Simulations indicate that BPAs

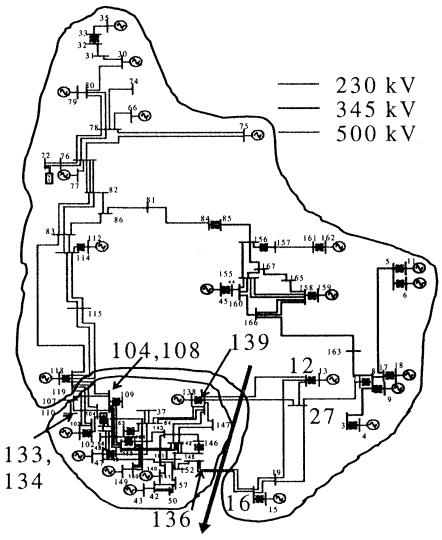

Fig. 8. Case 3—two islands for 179-bus system based on slow coherency.

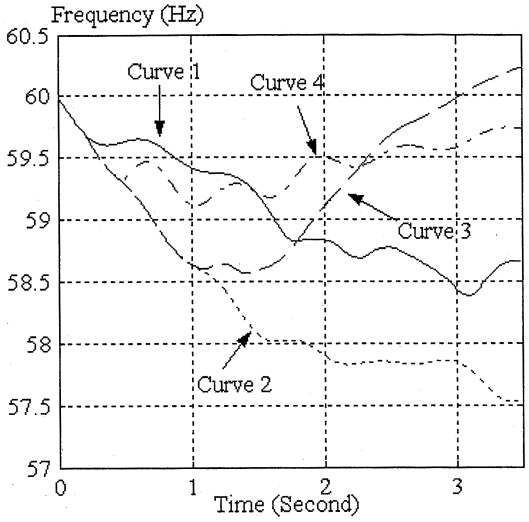

Fig. 9. Frequency response of generator 43 after the contingency of the 179-Bus system. Curve 1: Without self-healing. Curve 2: Islanding with no load shedding. Curve 3: Islanding followed by load shedding based on frequency difference. Curve 4: Islanding followed by the new load shedding.

R-Rdot out of step relays are able to quickly identify the out of step situation on those tie lines and initiate local and remote trippings. After islanding, the system is divided into three areas. These areas are shown in Fig. 6. The arrow shows the location where the three transmission lines are disconnected. The three islands in Fig. 6 can be characterized as the northeast island, the central island, and the south island. Fig. 7 shows the frequency responses of the same generator as in Fig. 5 in the central island in four situations.

The south island and the central island are load rich areas. The other island is the generation rich area. In the south island, all of the buses have mi less than m_0 and the conventional load shedding scheme is deployed. Simulations indicate that no load needs to be shed in the south island according to our load shedding scheme. The frequency recovers through the coordination of the generators' governors and exciters. In the central island, the new load shedding scheme is deployed. Similar conclusions can be obtained for this case as the previous one from the four frequency response curves.

In the third case, four lines are tripped simultaneously

1) bus 12–bus 139;
2) bus 27–bus 139;
3) bus 16–bus 136 (1and 2).

To save the system from an impending blackout, we split the system into two islands 0.2 s after the contingency. The islands are determined by the slow coherency. In order to create the island, the following lines are tripped:

1) bus 133–bus 108;
2) bus 134–bus 104.

The two islands are shown in Fig. 8. Fig. 9 shows the frequency responses of one typical generator in the south island in four situations. Table II shows the amount of load that needs to be shed for system recovery under the two load shedding schemes in the three cases considered.

In the cell that shows the amount of load shed, the first percentage is the ratio of the load shed compared to the total system load. The second percentage is the ratio of the load shed compared to the island load. It is observed that the load shedding scheme based on the rate of frequency decline sheds much less load than the conventional load shedding scheme in all three cases.

TABLE II
COMPARISON OF THE LOAD SHEDDING SCHEMES IN THREE CASES

Cases	Generation Load Imbalance (MW)	Load Shed with Conventional Scheme (MW)	Load Shed with New Scheme (MW)
No. 1	Generation 16,265 Load 22,679	6,937 (11.4% 30.6%)	5,698 (9.4% 25.1%)
No. 2	Central Island: Generation 5,118 Load 7,006 South Island: Generation 15,477 Load 17,373	1,810/0 (3.0%/0% 25.8%/0%)	1,450/0 (2.4%/0% 20.7%/0%)
No. 3	Generation 11,148 Load 15,674	5,127 (8.4% 32.7%)	3,672 (6.0% 23.4%)

V. CONCLUSION

In this paper, a self-healing scheme for large disturbances with concentration on a new load shedding scheme is described in detail. The scheme is tested on the 179-bus sample system and shows very good performance. The new two-level load shedding scheme raises the stability performance of the system by shedding less load compared to the conventional load shedding scheme. Since the tripping action does not require much calculations and the islanding information can be obtained offline, the speed in the real-time implementation should mostly depend on the speed of communication devices and switching actions. In order to facilitate restoration, the islands are formed by minimizing the generation-load imbalance. In this paper, we have not specifically addressed the topic of restoration. We will address this topic in our future work. In the future, we also intend

to do a detailed comparison of the new load shedding scheme with other standards reported in the literature.

ACKNOWLEDGMENT

The authors would like to thank Dr. M. Amin, Ram Adapa, EPRI, and Dr. R. Launer, DoD, for their leadership and guidance.

REFERENCES

[1] R. Brooks. (2001, Mar.) Web site on Subsumption Architecture. [Online]. Available: http://www.mit.edu/people/brooks.

[2] J. H. Chow, "Time-scale modeling of dynamic networks with applications to power systems," in *Lectures Notes in Control and Information Sciences*. Berlin, Heidelberg/New York: Springer-Verlag, 1982, vol. 46.

[3] M. Amin, C. C. Liu, G. T. Heydt, A. Phadke, and V. Vittal, "Development of analytical and computational methods for the strategic power infrastructure defense (SPID) system,", EPRI Annual Rep. Project WO-8333-01, Jan. 2001.

[4] J. R. Winkelman, J. H. Chow, B. C. Bowler, B. Avramovic, and P. V. Kokotovic, "An analysis of interarea dynamics of multi-machine systems," *IEEE Trans. Power Apparat. Syst.*, vol. PAS-100, pp. 754–763, Feb. 1981.

[5] R. Podmore, "Identification of coherent generators for dynamic equivalents," in *IEEE PAS-97*, 1978, pp. 1344–1354.

[6] P. V. Kokotovic, J. J. Allemong, J. R. Winkelman, and J. H. Chow, "Singular perturbations and iterative separation of time scales," *Automatica*, vol. 16, 1980.

[7] M. S. Tsai, "Development of islanding early warning mechanism for power systems," in *Power Eng. Soc. Summer Meeting*: IEEE, 2000, vol. 1, pp. 22–26.

[8] C. W. Taylor, J. M. Haner, L. A. Hill, W. A. Mittelstadt, and R. L. Cresap, "A new out-of-step relay with rate of change of apparent resistance augmentation," *IEEE Trans. Power Apparat. Syst.*, vol. PAS-102, pp. 631–639, Mar. 1983.

[9] J. M. Haner, T. D. Laughlin, and C. W. Taylor, "Experience with the R-Rdot out-of-step relay," *IEEE Trans. Power Syst.*, vol. PWRD-1, pp. 35–39, Apr. 1986.

[10] Z. Yang, "A new automatic under-frequency load shedding scheme," Master of Science thesis, Dept. of Electrical and Computer Engineering, Iowa State Univ. thesis, 2001.

[11] D. W. Smaha, C. R. Rowland, and J. W. Pope, "Coordination of load conservation with turbine-generator underfrequency protection," *IEEE Trans. Power Syst. Apparat. Syst.*, vol. PAS-99, pp. 1137–1145, May/June 1980.

[12] G. S. Grewal, J. W. Konowalec, and M. Hakim, "Optimization of a load shedding scheme," *IEEE Ind. Applicat. Mag.*, pp. 25–30, July/August 1998.

[13] C. J. Drukin, Jr., E. R. Eberle, and P. Zarakas, "An underfrequency relay with frequency decay compensation," *IEEE Trans. Power Apparat. Syst.*, vol. PAS-88, pp. 812–819, June 1969.

[14] A. A. Girgis and F. M. Ham, "A new FFT-based digital frequency relay for load shedding," *IEEE Trans. Power Apparat. Syst.*, vol. PAS-101, pp. 433–439, Feb. 1982.

[15] M. M. Elkateb and M. F. Dias, "New technique for adaptive-frequency load shedding suitable for industry with private generation," in *Proc. Inst. Elect. Eng. C*, vol. 140, no. 5, Sept. 1993.

[16] ——, "New proposed adaptive frequency load shedding scheme for cogeneration plants," in *Develop. Power Syst. Protection, 1993, Fifth Int. Conf.*.

[17] J. G. Thompson and B. Fox, "Adaptive load shedding for isolated power systems," *Proc. Inst. Elect. Eng.*, vol. 141, no. 5, Sept. 1994.

[18] P. M. Anderson and M. Mirheydar, "An adaptive method for setting underfrequency load shedding relays," *IEEE Trans. Power Syst.*, vol. 7, pp. 720–729, May 1992.

[19] P. M. Anderson and A. A. Fouad, *Power System Control and Stability*. Piscataway, NJ: IEEE Press, 1994.

[20] *American National Standard Requirements for Synchronous Machines*. New York: ANSI C50.10-1977, 1977.

[21] *IEEE Guide for Abnormal Frequency Protection of Power Generating Plants*. New York: IEEE Std. C37.106-1988, 1988.

[22] P. Kundur, *Power System Stability and Control*: McGraw-Hill, 1993, pp. 10–12.

[23] NPCC Emergency Operation Criteria.. [Online]. Available: http://www.npcc.org.

[24] S. Lindahl, G. Runvik, and G. Stranne, "Operational experience of load shedding and new requirements on frequency relay," in *Developments in Power Syst. Protection*, Mar. 25–27, 1997, Conf. Publication no. 434, IEE, pp. 262–265.

Haibo You (S'01) received the M.Sc. in engineering from Shanghai Jiaotong University, Shanghai, China, in 1999. He currently pursuing the Ph.D. degree in the Department of Electrical and Computer Engineering at Iowa State University, Ames.

He was with Xinhua Control Engineering Inc., Shanghai, China, focusing on distribution network automation. His research focuses on the area of control application in power system.

Vijay Vittal (S'78–F'97) received the B.E. degree in electrical engineering from Bangalore, India, in 1977, the M.Tech. degree from the Indian Institute of Technology, Kanpur, India, in 1979, and the Ph.D. degree from Iowa State University, Ames, IA, in 1982.

Currently, he is the Harpole Professor in the Electrical and computer engineering department at Iowa State University.

Dr. Vittal is the recipient of the 1985 Presidential Young Investigator Award and the 2000 IEEE Power Engineering Society Outstanding Power Engineering Educator Award.

Zhong Yang received the B.Sc. degree from Tsinghua University, Beijing, China, in 1998, and the M.Sc. degree in electrical engineering from Iowa State University, Ames, in 2001.

Currently, he is with GE Power System Control, Melbourne, FL.